

Depth And Surface Roughness Control On Laser Micromachined Polyimide For Direct-Write Deposition

B. Pratap¹, C.B. Arnold^{2*} and A. Piqué²

¹Department of Mechanical and Aerospace Engineering, The George Washington University, 801 22nd Street NW, Washington DC 20052, USA

²Materials Science and Technology Division, Code 6372, Naval Research Laboratory, Washington DC 20375, USA

Abstract

We are examining surface characteristics of ultraviolet pulsed-laser micromachined structures in polyimide as a function of the incident laser energy and the distance between subsequent laser spots in order to prepare surfaces for laser direct-write deposition of metals. Variations in the spot-to-spot translation distance provide an alternative means of average depth and roughness control when compared to fluence changes and focal distance variations. We find that the average depth is proportional to the inverse of the translation distance, while the root mean square surface roughness reaches a minimum when the translation distance is approximately equal to the full width half maximum of a single ablation mark on the surface. Conductive silver metal lines are deposited on the surface machined features demonstrating the ability to produce conductors with good adhesion over stepped structures on polyimide.

Keywords: pulsed laser micromachining, laser forward transfer, polyimide

1. INTRODUCTION

Pulsed laser micromachining has emerged as a powerful tool in scientific and industrial applications where the need for high aspect ratio features and accurate depth control is not met by conventional patterning techniques.¹ A key advantage of laser micromachining over other conventional patterning or etching techniques is the ability to remove materials ranging from ceramics and metals to semiconductors and polymers without the need to change tooling or chemical processing. Typical applications include drilling through vias,² ink jet printer nozzle drilling,³ microscopic channels,⁴ direct-write patterning,⁵ surface cleaning^{6, 7} and retexturing.⁸ More recent developments in microelectromechanical systems (MEMS) fabrication have used ultraviolet (UV) laser micromachining to locally remove a polymer sacrificial layer in order to release the desired feature without the need for additional wet chemical processing.^{9, 10}

Pulsed laser micromachining forms an integral part of many micro-fabrication and manufacturing processes and enables a large degree of flexibility in materials processing by introducing a variety of parameters to control the roughness and depth of the micromachined structures. Examples of these parameters include incident laser fluence, position of focal plane, laser spot size and translation distance between subsequent laser pulses. In fact, due to the large number of parameters, the laser micromachining process is rarely optimized, but rather adjusted by trial-and-error, which tends to be time consuming and cost ineffective.¹¹ Typically, the depth

* Corresponding author: Phone: +1-202-404-2093, E-mail: craig.arnold@nrl.navy.mil

and roughness of micromachined structures are adjusted by changing the laser fluence; however, optimization is difficult due to the secondary issues that arise when the fluence is changed, such as increased debris formation, energy transients, or additional equipment required for continuous fluence control. Furthermore, the depth as function of laser energy does not obey a single relation over all energy regimes and thus necessitates the trial-and-error approach to obtain the desired results.^{12, 13}

Spot-to-spot translation distance as a means to control depth and surface roughness helps eliminate the issues associated with fluence change techniques and avoids the need to machine at higher energies that tends to result in greater debris generation.¹⁴ Furthermore, translation distance in a micromachining setup can be continuously modified during the process by simple computer control of either a substrate stage or a rastering mirror.

The effects of translation distance on micromachining are clearly demonstrated in the model system of polyimide. In this well-studied system, the ablation mechanism is consistent with a photochemical desorption model whereby the laser pulses directly initiate the breaking of chemical bonds forming volatile by-products.¹⁵⁻¹⁷ As a result, polyimide exhibits relatively low heat dissipation with little debris formation, in contrast to other systems, such as silicon, that ablate through a photo-thermal interaction which produces increased surface roughness and larger heat affected regions.¹⁸⁻²⁰

Polyimide, as a technical system, meets requirements for use in the electronics industry for thermal and mechanical stability as a substrate material or an insulating layer.¹² Depth control in polyimide micromachining is extremely important in applications where an underlying metallic layer must be exposed, undamaged, for grounding purposes or through vias.²¹ However, one of the problems with polyimide as a substrate for electronic materials is the difficulty in producing conductive lines with good adhesion on the surface. Standard polyimide substrates are typically bonded to electroplated materials to produce conductive ground planes that can be subsequently etched or machined to create lines. As an alternative to bonded layers, micromachined polyimide can be used as a template for subsequent deposition through other techniques such as laser direct-write.^{22, 23} In these cases, the controlled depth and morphology are critical to the electrical conductivity and adhesion of the deposited materials.

In the present study, trenches are micromachined in polyimide at various translation distances and laser energies and the resultant depth and root mean square (RMS) surface roughness is examined. We find a simple relationship between the average depth and the translation distance that is maintained over the entire range of translation distances used in this study. The results are used to produce a sample 3-D structure in the form of a stepped pathway on which conductive silver is conformally deposited with good adhesion.

2. EXPERIMENTAL SETUP

The laser micromachining experimental setup is shown in figure 1. The pulsed UV laser source for these experiments is a Nd:YVO₄ laser (Spectra Physics) operating at 355 nm with a frequency of 10 KHz and a pulse duration of 30 ns. The laser pulse passes through a series of focusing optics and a UV microscope objective before reaching the sample which is mounted on a vacuum chuck. The nominal laser spot size in this setup is 25 μm in diameter. All the samples

are irradiated at energies ranging from 3-30 μJ per pulse ($\sim 2\text{-}20 \text{ J/cm}^2$) with internal laser fluctuations of $\pm 5\%$ as measured by an energy-meter (Ophir Nova) monitoring the laser pulse energy during the experiment.

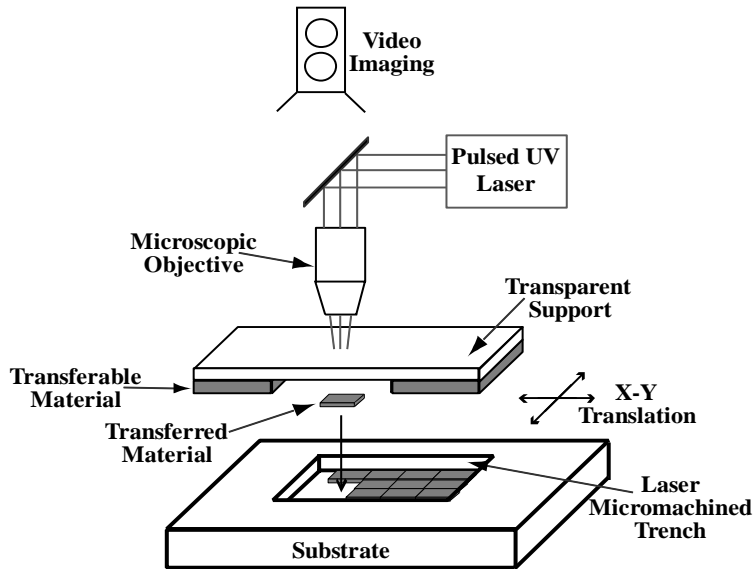


Figure 1. Schematic illustrating the elements of the laser micromachining and deposition apparatus.

The spot-to-spot translation distance is controlled by an x-y motion control system (Aerotech D500) with a maximum x velocity of 115 mm/s and y velocity of 100 mm/s. A schematic of the resulting laser machined pattern is shown in figure 2. An acousto-optic modulator (NEOS) is used to fix the dwell time between subsequent laser pulses. For all the experiments shown here, the time between pulses is 10 ms to allow for efficient stage operation and avoid cumulative heating effects. Inline video imagery enables sample alignment as well as real time monitoring of the micromachining process.

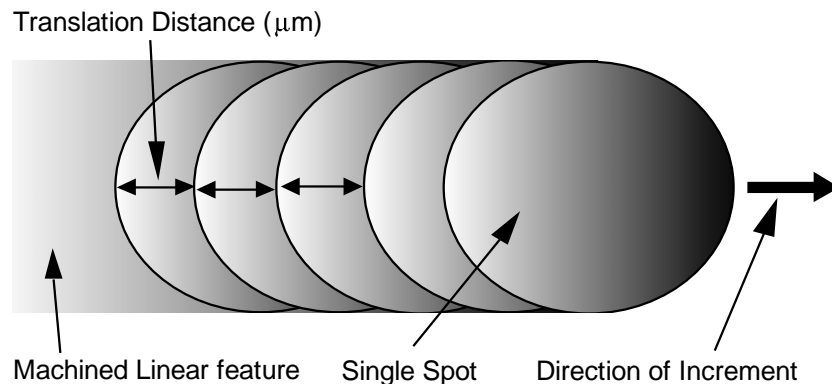


Figure 2. Schematic picture of the translation distance controlled by stage velocity.

In the present study polyimide (110 μm thick DuPont KaptonTM Type H) samples are irradiated at varying translation distances and laser energies. Substrates are cleaned with acetone and ethanol prior to laser micromachining. Using a laser spot 25 μm -wide, square frames 500 μm x 500 μm are machined on these polyimide substrates with translation distances ranging from 1 μm to 40 μm . All experiments are performed at room temperature and ambient pressure where it has been shown that atmospheric conditions have no measurable influence on pulsed UV laser micromachining of polyimide.²⁴

The same apparatus is used to deposit conductive silver lines using a laser forward transfer direct-write technique described elsewhere.^{22, 23} A commercially available screen printing silver ink (Paralec Inc.) is spread in a 10 μm thick layer on a borosilicate blank that is then mounted above the machined substrate. The laser interacts with the ink and causes a forward transfer of material that lands on the waiting substrate 100 μm below. For deposition, the spot size is increased to 120 μm giving us a decreased laser fluence of $\sim 0.6 \text{ J/cm}^2$. Conformal deposition over a variety of surface structures is easily obtained. Following deposition, the transferred ink is dried in an oven at 150 $^\circ\text{C}$ for 5 minutes.

Surface characterization measurements are performed on samples after laser irradiation and after laser deposition without any additional substrate cleaning to preserve the surface structure. Depth and surface roughness measurements are performed using a profilometer (Tencor Instruments P-10) with a 2 μm stylus tip. Measurements of machined features are sampled over a fixed distance of 450 μm on one side of the machined frame. In all cases, the same side of the frame is used to prevent errors associated with starting and stopping or asymmetric spot geometries. Scanning electron microscopy (LEO 1550) is performed to further investigate surface features in polyimide after laser irradiation.

3. RESULTS

Figure 3 shows a SEM image of a polyimide substrate laser irradiated at 7 μJ with a translation distance of 15 μm . Translation occurs from right to left in a straight line across the image. The machined groove exhibits a smooth central region with secondary fringe formation around the circumference of each laser spot. At this translation distance there is significant

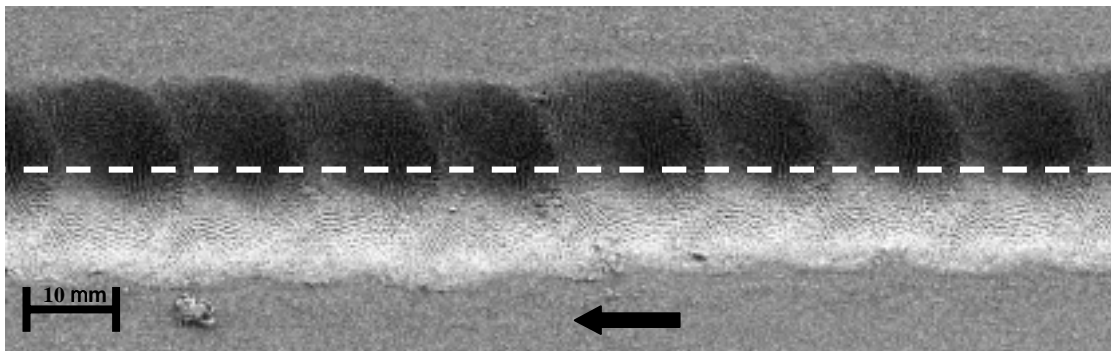


Figure 3. Micromachined channel in polyimide at a translation distance of 15 μm and pulse energy of 30 μJ . Arrow indicates the direction in which the sample is translated, while the dotted line shows the typical region measured with a profilometer to determine depth and surface roughness.

overlap between spots that leads to a continuous groove in the polyimide. Figure 4 shows plots of the depth, measured by surface profilometry, along the machined channel for constant energy and different translation distances. The data was acquired from the central region of the structure as depicted in figure 3, and the average depth for both plots is indicated by a dashed line. For both translation distances in figure 4, the energy is 30 μJ , however, at a translation distance of 10 μm (figure 4b), the RMS roughness is less and the average depth is greater than at a translation distance of 40 μm (figure 4a). Relatively smooth sections between the ridges in figure 4a indicate very little debris formation during the machining process. If we focus on a single ablation spot, we find the full width half maximum (FWHM) to be $\sim 14 \mu\text{m}$. Figure 4b shows

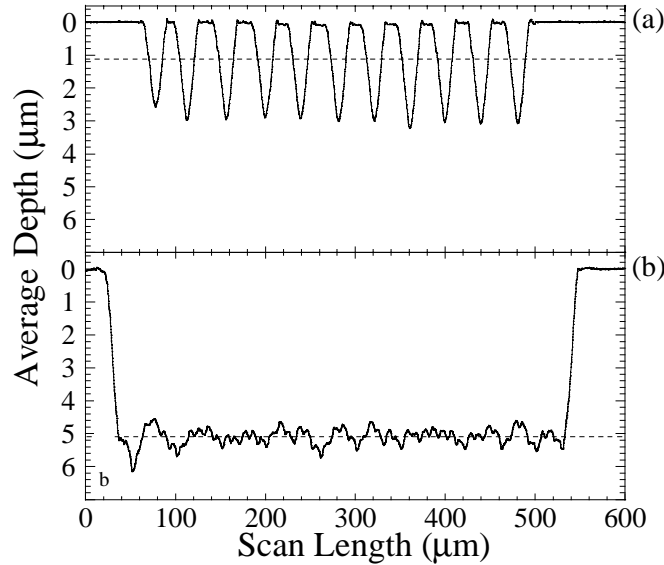


Figure 4. Change in average depth induced by change in translation distance at constant energy. (a) Profilometer line scan of a sample micromachined at 40 μm shows decreased average depth as compared to (b) micromachined at 15 μm translation distance. Both samples are irradiated at 30 μJ . The full width half maximum (FWHM) $\sim 14 \mu\text{m}$ is denoted in (a).

periodic behavior with two underlying length scales. The structures with the shorter period ($\sim 10 \mu\text{m}$) are due to the translation distance of incident laser pulse, while we attribute the structures with longer period ($\sim 50 \mu\text{m}$) to fluctuations in laser energy. The change in average depth and surface roughness in these cases is brought about solely by the change in translation distance.

Figure 5 depicts a semi-log plot of average depth as a function of translation distance at constant energies of 3 μJ , 16 μJ and 30 μJ . The average depth R_a is calculated as:

$$R_a = \frac{1}{L} \int_0^L |y(x)| dx \quad (1)$$

where, L is the scan length (450 μm) and y the scan depth as a function of position x . For all fixed laser energies, the average depth increases as the translation distance is decreased. Figure 5 shows that at 3 μJ , the average depth, h , follows the relation:¹

$$h = \frac{A}{\Delta} \quad (2)$$

where, A is a fitting parameter that depends on the laser energy and Δ is the translation distance. At higher energies, the average depth follows the same behavior for depth below 9 μm , however, at greater depths, the data diverges from the expected behavior. This effect is caused by a limitation in our profilometer apparatus to measure high aspect ratio features due to the stylus geometry. However, the simple dependence between average depth and translation distance makes it possible to accurately laser micromachine polyimide to a predictable and predetermined average depth.

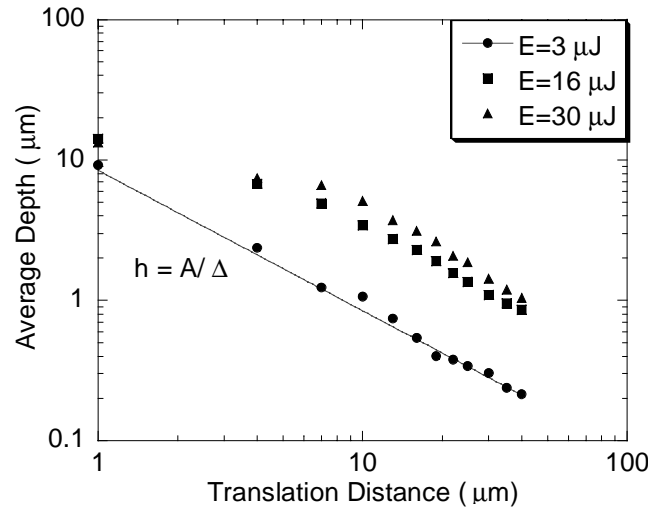


Figure 5. Dependence of average depth as a function of translation distance. Change in average depth is observed at three constant energies at translation distances ranging from 40 μm to 1 μm . The solid line shows a fit to A/Δ with $A=9.2 \mu\text{m}^2$.

Figure 6 shows a plot of RMS roughness as a function of varying translation distance at a constant laser energy of 27 μJ . The RMS roughness, R_q , is calculated as:

$$R_q = \sqrt{\frac{1}{L} \int_0^L (y(x) - R_a)^2 dx} \quad (3)$$

where again, L is the scan length and y is the scan depth, and R_a the average depth given by equation 1. At large translation distances, the RMS roughness gradually decreases until a sharp decrease in roughness occurs which is associated with the introduction of spot-to-spot overlap at smaller translation distances. We find this decrease in roughness to slow for translation distances less than the FWHM of 14 μm as measured in figure 4. Optimization of surface

roughness can be desirable in applications where properties such as adhesion, chemical activity, or interfacial features, play an important role. Our results show that the translation distance can be used as a simple means to vary and optimize the surface roughness in polyimide.

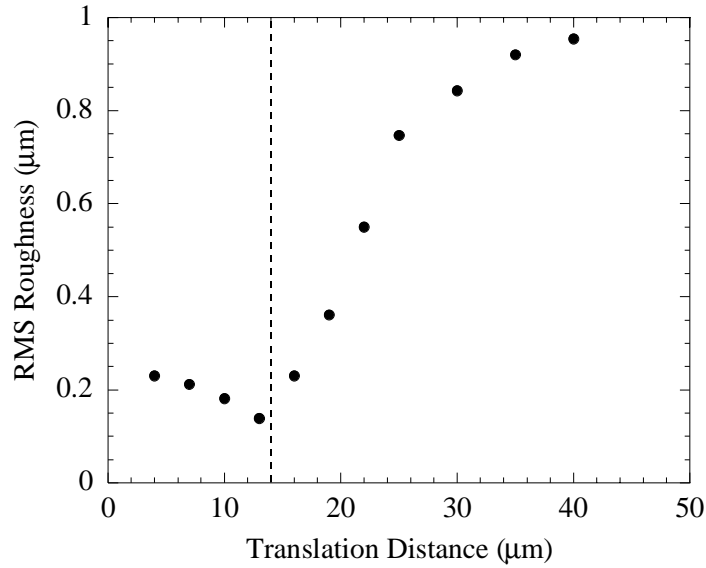


Figure 6. RMS roughness as a function of translation distance at 27 μJ. Roughness decreases with reducing translation distance and reaches a minimum when the translation distance approximately equals the laser FWHM spot size.

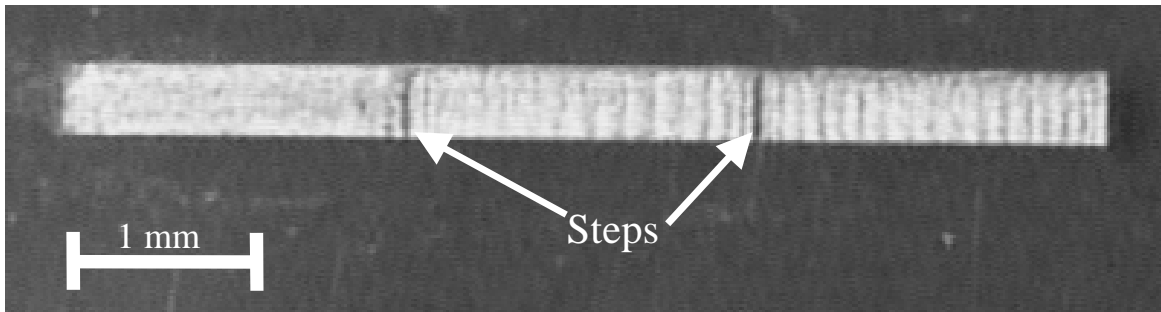


Figure 7. Micrograph of concentric terraces micromachined in polyimide at a laser energy of 30 μJ and different translation distances. Silver is laser forward transferred over the steps producing a continuous 30 μm thick layer.

Figure 7 shows an example of a machined terrace structure in polyimide that has been generated by adjusting the translation distance at fixed laser energy of 30 μJ. The image clearly shows three distinct terraces corresponding to depths of 30, 60, and 100 μm. Using the laser direct-write technique, we conformally deposit silver over the stepped surface producing a layer that is on average 30 μm thick above the flat regions of the structure. The adhesion of the film is verified by surviving a scratch test using a #2 pencil. A four-point measurement of the resistance

from one end to the other shows the deposited film is continuous across the step edges with a resistance of 0.8Ω . Since the film thickness is not constant across the step edges, there is higher resistance across the step edges in comparison to the resistance across a single flat region, which makes the actual resistivity of the film difficult to determine. A rough estimate assuming the average thickness of $30 \mu\text{m}$ yields a resistivity 100x bulk, but further characterization needs to be done to determine the thickness of the deposited material on the step edges and thereby the resistivity of the laser deposited silver.

4. CONCLUSIONS

Change in translation distance is a convenient alternative to depth control mechanism for pulsed laser micromachining of polyimides. It is observed that the average depth is inversely proportional to the translation distance over two orders of magnitude making it possible to accurately predict the average machined depth for a given energy. By varying the translation distance, it is also possible to control the surface roughness of the micromachined structures. Our results show the surface roughness is minimized at translation distances less than the full width half maximum of the laser spot. Laser forward transfer direct-write is used to deposit silver conformally on 3-D laser micromachined trenches in polyimide produced by varying translation distance and the resultant films show good adhesion and conductivity. Future work in controlling laser micromachined structures for characterizing and optimizing the properties of laser deposited conductive material is ongoing.

5. ACKNOWLEDGEMENTS

We thank Dr. S. Lakeou for helpful discussion and E. Coakley for assistance. This research was supported by the Office of Naval Research. In addition, CBA acknowledges the support of the National Research Council Postdoctoral Associate Program.

6. REFERENCES

- 1 S. Metev and V. Veiko, *Laser Assisted Microtechnology*, Springer-Verlag, Berlin, 1994
- 2 P. M. Martin, D. W. Matson, W. D. Bennett, Y. Lin, and D. J. Hammerstrom, *J. Vac. Sci. Technol., A*, **17**, 2264 (1999)
- 3 M. C. Gower, *Optics Express*, **7**, 56 (2000)
- 4 S. J. Qin and W. J. Li, *Sens. Act. A*, **97-98**, 749 (2002)
- 5 H. Helvajian, "3d Microengineering via Laser Direct-Write Processing Applications", *Direct Write Techniques for Rapid Prototyping Applications*, Alberto Piqué, Douglas B. Chrisey, p. 415, Academic Press, San Diego, 2002
- 6 A. C. Tam, H. K. Park, and C. P. Grigoropoulos, *Appl. Surf. Sci.*, **127-129**, 721 (1998)
- 7 K. Coupland, P. R. Herman, and B. Gu, *Appl. Surf. Sci.*, **127-129**, 731 (1998)

- 8 J. J. Yu, J. Y. Zhang, and I. W. Boyd, *Appl. Phys. A*, **72**, 687 (2001)
- 9 A. S. Holmes, *RIKEN Review*, **43**, 63 (2002)
- 10 A. S. Holmes and S. M. Saidam, *J. Microelectromech. Sys.*, **7**, 416 (1998)
- 11 V. N. Tokarev, J. Lopez, and S. Lazare, *Appl. Surf. Sci.*, **168**, 75 (2000)
- 12 J. R. Sobehart, *J. Appl. Phys.*, **74**, 2830 (1993)
- 13 E. Sutcliffe and R. Srinivasan, *J. Appl. Phys.*, **60**, 3315 (1986)
- 14 R. Srinivasan, *Appl. Phys. Lett.*, **58**, 2895 (1991)
- 15 R. Srinivasan, B. Baren, and R. W. Dreyfus, *J. Appl. Phys.*, **61**, 372 (1987)
- 16 R. Srinivasan, "Ultraviolet Laser Ablation of Organic Polymer Films", *Laser Processing and Diagnostics*, D. Bäuerle, p. 343, Springer-Verlag, New York, 1984
- 17 R. Srinivasan and B. Braren, *J. Polym. Sci. A*, **22**, 2601 (1984)
- 18 P. E. Dyer and J. Sidhu, *J. Appl. Phys.*, **57**, 1420 (1985)
- 19 J. E. Andrew, R. E. Dyer, D. Forster, and P. H. Key, *Appl. Phys. Lett.*, **43**, 717 (1983)
- 20 T. S. Selinger, D. G. Cahill, S. C. Chen, S. J. Moon, and C. P. Grigoropoulos, *Phys. Rev. B*, **64**, 155323-1 (2001)
- 21 P. Metayer, J. Davenas, and J. M. Bureau, *Nucl. Instr. and Meth. Phys. Res. Sect. B*, **185**, 156 (2001)
- 22 D.B. Chrissey, A. Piqué, J. Fitz-Gerald, R.C.Y. Auyeung, R.A. McGill, H.D. Wu, M. Duignan, *Appl. Surf. Sci.* **1-4**, 345 (2000)
- 23 A. Piqué, D.B. Chrissey, R.C.Y. Auyeung, S. Lakeou, R. Chung, R.A. McGill, P.K. Wu, M. Duignan, J. Fitz-Gerald and H.D. Wu, *SPIE Proceedings*, **3618**, p. 330 (1999)
- 24 J. H. Branon, J. R. Lankard, A. I. Baise, F. Burns, and J. Kaufman, *J. Appl. Phys.* **58**, 2036 (1985)